Available online at www.sciencedirect.com
ScienceDirect
Natural Gas Industry B 3 (2016) 146−151

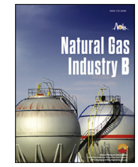

www.elsevier.com/locate/ngib

Research article

A new post-frac evaluation method for shale gas wells based on fracturing curves ☆

Bian Xiaobing [a,b,*], Jiang Tingxue [a,b], Jia Changgui [a,b], Wang Haitao [a,b], Li Shuangming [a,b], Su Yuan [a,b], Wei Ran [a,b]

[a] *Sinopec Research Institute of Petroleum Engineering, Beijing 100101, China*
[b] *Shale Gas Enrich Pattern and Effectively development of State Key Lab, Chaoyang district, Beijing 100101, China*

Received 31 October 2015; accepted 16 March 2016
Available online 27 August 2016

Abstract

Post-fracturing evaluation by using limited data is of great significance to continuous improvement of the fracturing programs. In this paper, a fracturing curve was divided into two stages (i.e., prepad fluid injection and main fracturing) so as to further understand the parameters of reservoirs and artificial fractures. The brittleness and plasticity of formations were qualitatively identified by use of the statistics of formation fracture frequency, and average pressure dropping range and rate during the prepad fluid injection. The composite brittleness index was quantitatively calculated by using the energy zones in the process of fracturing. It is shown from the large-scale true triaxial physical simulation results that the complexity of fractures is reflected by the pressure fluctuation frequency and amplitude in the main fracturing curve, and combined with the brittleness and plasticity of formations, the fracture morphology far away from the well can be diagnosed. Well P, a shale gas well in SE Chongqing, was taken as an example for post-fracturing evaluation. It is shown that the shale beds are of stronger heterogeneity along the extension directions of horizontal wells, and with GR 260 API as the dividing line between brittleness and plasticity in this area, complex fracture systems tend to form in brittleness-prone formations. In Well P, half of the fractures are single fractures, so it is necessary to carry out fine subsection and turnaround fracturing so as to improve development effects. This paper provides a theoretical basis for improving the fracturing well design and increasing the effective stimulated volume in this area.

Keywords: Shale gas well; Post-frac evaluation; Prepad fluid injection; Main fracturing; Brittleness; Fracture complexity; Quantitative evaluation; SE Chongqing

Shale matrix has extremely low porosity and permeability, and contains abundant adsorbed gas; therefore, shale gas is characterized by a long recovery life and a long production cycle [1−4]. In a shale gas block of SE Chongqing, the costs of well drilling, completion and fracturing are high, ranging from RMB 7000 × 10^4 to 9000 × 10^4 yuan, and the stable gas production is 1 × 10^4−2 × 10^4 m^3/d. In order to control the costs, many supporting measures (e.g. conventional logging, fracture morphology monitoring and tests of gas production profile) have been less-frequently implemented [5−7]. The post-fracturing evaluation method based on a mature software model can provide multiple solutions and requires interpretable data. For instance, the G function analytical method based on the pressure decline curve after the pump is stopped requires the pressure test data after a long period of pump stop; the interpretation can't be achieved if the time of pressure test in field is short. Therefore, the reliability of post-fracturing evaluation results is directly related to the evaluator's

☆ Project supported by the National Natural Science Funds "Mechanism of dynamic stochastic fracture control and theory of waterless fracturing for shale formations" (Grant No. 51490653), the Sinopec S&T Researches "Optimal stimulation technology for shale gas formations in Fuling Block" (Grant No. P14091), and the National Major S&T Projects "Demonstration of shale gas exploration and development under normal pressure in Pengshui region" (Grant No. 2016ZX05061).
* Corresponding author.
E-mail address: xiaobingbian@126.com (Bian XB).
Peer review under responsibility of Sichuan Petroleum Administration.

http://dx.doi.org/10.1016/j.ngib.2016.03.010

experience [8−10]. How to further accurately understand shale formation based on limited data has been a conundrum for researchers. The authors proposed a new method that can invert the reservoir parameters and qualitatively evaluate fracture morphology of post-fracturing based on fracturing curves. With this method and through full use of the data of stimulated wells, the fracture and reservoir parameters can be re-understood. Taking a shale gas well, Well P, in SE Chongqing as an example, the post-fracturing evaluation was performed, providing theoretical basis for further amelioration of fracturing design and improvement of effective stimulated reservoir volume.

1. Overview of stimulated wells

Well P in a shale gas block of SE Chongqing was obliquely drilled to 4190 m in the Lower Silurian Longmaxi Fm, with a horizontal section of 1260 m. A total of 22 intervals were fractured, with 2−3 clusters per interval. The maximum displacement of fracturing maintained at 13.0−14.5 m^3/min, the mean pressure of fracturing ranged from 60 to 70 MPa, total fluid volume reached 46542 m^3, and total sand volume was 2108 m^3.

According to the gradient of instantaneous initial shut-in pressure (*ISIP*) in formation and the existence of formation leakage (leakage zone encountered in the first 6 intervals), the fracturing pressure curve can be divided into four types: Type 1, Intervals 1−2, leaking formation, *ISIP* = 0.021−0.023 MPa/m; Type 2, Intervals 3−7, leaking formation, *ISIP* = 0.016−0.017 MPa/m; Type 3, Intervals 8−13, non-leaking formation, *ISIP* = 0.018−0.022 MPa/m; Type 4, Intervals 14−22, non-leaking formation, *ISIP* = 0.023−0.026 MPa/m. As shown in Fig. 1, Well P shows higher crustal stress at about 100 m to the toe side, and gradually-increased crustal stress to the heel side.

2. Identification of formation brittleness and plasticity

In the process of fracturing of a shale gas well, fractures are continuously initiated and propagated as prepad fluid is injected into the formation. Brittleness and plasticity of shale formation were identified depending on pressure dropping range and rate at the fracturing pressure points.

2.1. Characterization of formation fracturing

Interval 5 of Type 2 in the fracturing curve (Fig. 2) was selected to analyze the formation fracturing pressure characteristics in the prepad fluid stage trapped by the red rectangular dash circle. This interval presents a leaking formation with low crustal stress. In the process of displacement increase and a state with larger displacement, the formation was fractured, showing clear pressure dropping range of 2.1−5.2 MPa and rate of 1.68−6.67 MPa/min at three points. The large pressure dropping range and rate after fracture initiation indicates good brittleness, large fluid loss, and good existence of natural fractures in the formation.

Similarly, the formation fracture frequency, mean pressure dropping range and rate in the displacement increase stage were counted for 22 intervals in Well P (Table 1). In Intervals 1−6, abundant natural fractures existed, and pressure dropping range and rate were high; several periods of obvious fracturing occurred in the process of displacement, implying that the formation is brittleness-prone. In Intervals 7−11, pressure dropping range and rate were low, 2−3 periods of minor fracturing occurred at relatively low displacement, implying that the formation is plasticity-prone. In Intervals 12−22, due to higher crustal stress, pressure dropping rate decreased to some extent, and the frequency of obvious fracturing decreased, implying that the formation has medium plasticity and brittleness.

2.2. Quantitative evaluation of formation brittleness and plasticity

For plastic shale formation, the pressure is almost constant after fracturing, but continual deformation results in large energy consumption. For brittle shale formation, the pressure drops rapidly after fracturing, and the energy consumption is relatively small. With the method proposed in Ref. [11], the energy zone at fracture initiation in the process of fracturing

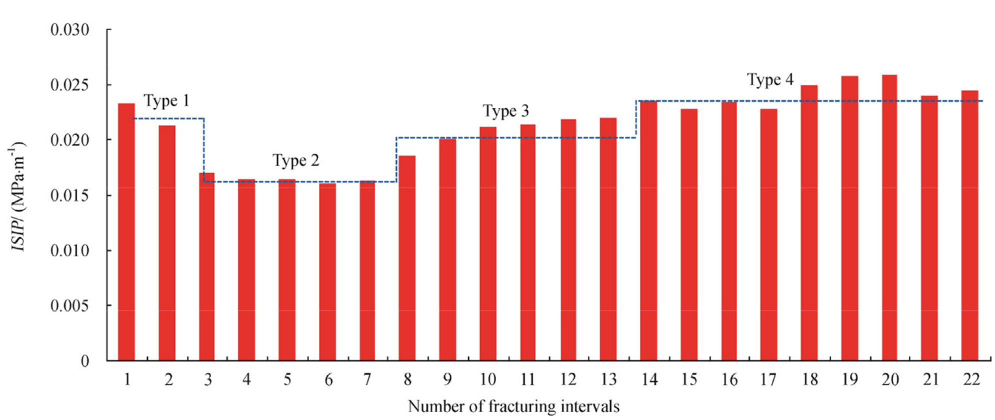

Fig. 1. Division of fracturing pressure curve for the given well.

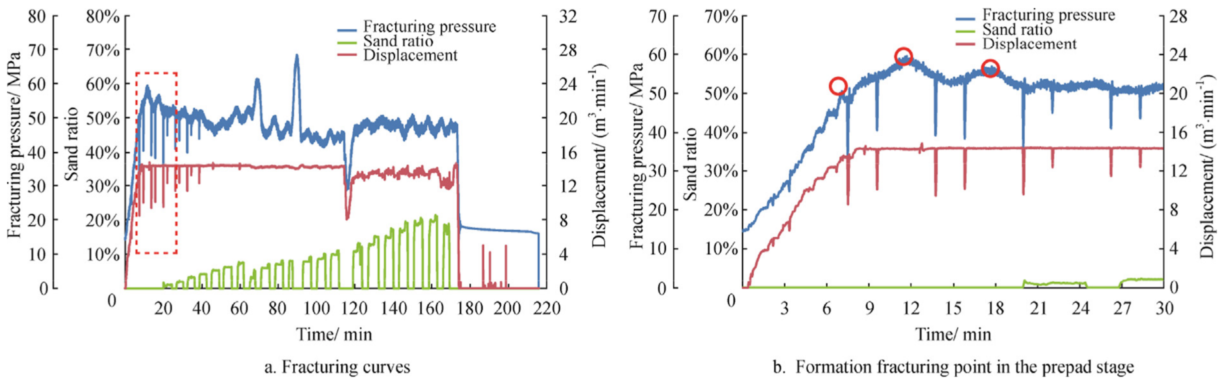

Fig. 2. Data of fracturing for Interval 5.

was used to characterize the composite brittleness index. The expression is given below:

$$BI=\frac{(T_c-T_0)(p_{max}+p_h-p_f)-\int_{T_0}^{T_c}(p(t)+p_h-p_f)dt}{(T_c-T_0)(p_{max}+p_h-p_f)} \quad (1)$$

where BI represents the composite brittleness index of shale; $p(t)$ represents wellhead pressure, MPa; p_{max} represents the fracturing pressure at the shale wellhead, MPa; p_h represents hydrostatic pressure, MPa; p_f represents the friction pressure along the wellbore, MPa; T_c represents the time when the pressure drops to the minimum value after fracturing, min; T_0 represents the time when the pressure rises to a maximum value after deformation of formation, min.

The composite brittleness index was calculated for Well P, as shown in Table 2. It is seen that the index is 30.9−54.3%, suggesting that the shale formation penetrated by the horizontal interval has strong heterogeneity.

2.3. Comprehensive evaluation of formation brittleness and plasticity

On the whole, the natural gamma (GR) value of the perforation location of the horizontal interval in Well P and the formation fracturing characteristics of the fracturing pressure curve in each interval have certain correlations. Firstly, when the GR value is 150−260 API, the mean fracturing frequency is 4.1 times, the mean pressure dropping range is 3.9 MPa, the mean pressure dropping rate is 13.1 MPa/min, and the mean brittleness index is 40.1%. Secondly, when the GR value is greater than 260 API, the mean fracturing frequency is 2.4 times, the mean pressure dropping range is 2.0 MPa, the mean pressure dropping rate is 9.7 MPa/min, and the mean brittleness index is 35.8%. As for the shale gas well in this block, the brittleness and plasticity of the formation penetrated by the horizontal interval can be diagnosed according to the GR value, so as to provide a basis for fracturing design of each interval.

Table 1
Data of formation fracturing characteristics for 22 intervals in Well P.

Perforation interval	*GR*/API	Fracturing times	Displacement/($m^3 \cdot min^{-1}$)	Dropping range of mean pressure/MPa	Dropping rate of mean pressure/($MPa \cdot min^{-1}$)
1	243	7	5.5−11.0	3.7	17.4
2	244	6	4.0−12.2	4.7	34.5
3	259	12	0.9−13.2	4.0	29.5
4	245	7	5.7−13.0	1.9	8.4
5	210	3	10.0−14.4	4.2	4.7
6	248	5	4.0−14.1	3.6	17.4
7	370	3	3.5−6.0	0.9	15.0
8	431	2	5.0−9.3	1.8	8.2
9	388	2	7.4−9.5	2.4	6.9
10	413	3	2.7−6.6	2.4	9.1
11	235	4	2.7−13.3	4.3	25.8
12	231	3	2.5−4.8	2.2	8.2
13	389	2	1.4−2.3	2.7	9.5
14	187	4	1.8−2.7	4.0	18.4
15	180	3	0.7−2.8	4.2	6.8
16	200	1	2.7	1.5	10.0
17	240	1	2.3	8.8	7.3
18	228	2	5.7−13.4	3.8	2.4
19	242	2	1.8−3.0	2.6	8.0
20	242	2	2.8−13.4	4.3	1.2
21	248	4	1.0−13.6	4.2	15.7
22	156	3	5.8−13.4	4.2	7.4

Table 2
Brittleness index for intervals in Well P.

Perforation interval	1	2	3	4	5	6	7	8	9	10	11
Brittleness index	36.2%	38.5%	39.8%	33.1%	48.9%	38.9%	30.9%	34.4%	34.6%	43.9%	35.0%
Perforation interval	12	13	14	15	16	17	18	19	20	21	22
Brittleness index	33.7%	35.4%	32.4%	33.6%	47.0%	48.5%	35.3%	42.4%	43.7%	54.3%	39.9%

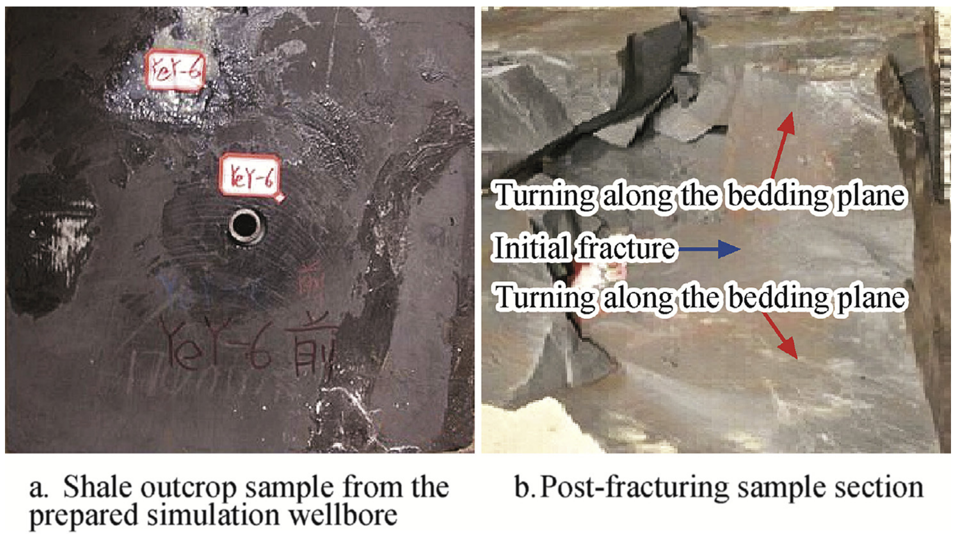

Fig. 3. Physical simulation experiment of shale outcrop.

3. Comprehensive evaluation of complex fracture morphology

3.1. Large physical simulation experiment

A large number of hydraulic fracturing physical simulation experiments were conducted on a 300 mm × 300 mm × 300 mm shale outcrop under the condition of true triaxial compression. Post-fracturing monitoring shows the existence of both complex and single fractures. Taking the typical rock sample with complex fractures as an example (Fig. 3), the outcrop sample from the prepared simulation wellbore shows good integrity, with only a minor of unpenetrated natural fractures along the natural bedding. The stress in three directions was respectively set as follows: $\sigma_v = 20.4$ MPa, $\sigma_H = 18.4$ MPa, and $\sigma_h = 14.7$ MPa, and the pump displacement was 0.5 mL/s. Red tracing agent was added in the fracturing fluid to trace the fracture propagation state. The post-fracturing sample section shows that fractures formed after fracturing interweave with the open natural bedding plane, thus forming a fracture network system. In Fig. 4, the results of acoustic emission real-time monitoring validates that the shale in this block possesses a basis for the formation of complex fractures.

3.2. Morphology of pressure curves

The pressure drop after the pump was stopped was tested for only four intervals in Well P. Therefore, the diagnosis of fracture morphology in each interval can't be managed through G function analysis. Large physical simulation experiment shows that higher fluctuation frequency in the fracturing curve corresponds to higher pressure drop, the signal from acoustic emission monitoring ranges more extensively, and a more complex fracture pattern occurs. Based on the observation described above, pressure fluctuation frequency and mean pressure amplitude were collected by eliminating the influence of density difference in the sand-carrying fluid at the slick-water hydraulic fracturing stage in Well P, and the expression for bottomhole pressure is as follows [12]:

$$p_b = p_w + p_h - p_f \quad (2)$$

where p_b represents bottomhole pressure, MPa; p_w represents wellhead pressure, MPa.

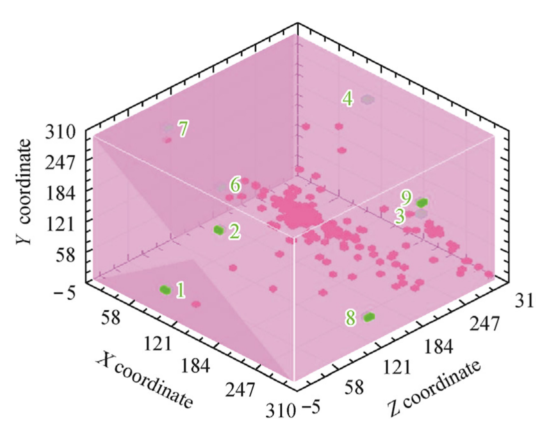

Fig. 4. Acoustic emission real-time monitoring results.

Table 3
Pressure fluctuation times and amplitude of representative intervals in Well P.

Type	Representative intervals	Pressure fluctuation frequency	Pressure fluctuation amplitude/MPa	Fracture developmental degree
1	2	10	6–8 MPa for 5 amplitudes, 3–5 MPa for the others	Far-well fractures are relatively developed, and natural fractures are widely distributed
2	5	18	Higher than 4 MPa for 9 amplitudes (up to 9 MPa and 22 MPa for two), about 1.5 MPa for the others	Far-well fractures are relatively developed, and natural fractures are widely distributed
3	8	7	Higher than 4 MPa for only 5 amplitudes, less than 2 MPa for the others	Fractures are not relatively developed, and natural fractures are distributed in limited areas
4	18	12	4–5 MPa for 6 amplitudes, about 3 MPa for the others	Formation is homogeneous, with fractures which are distributed in limited areas

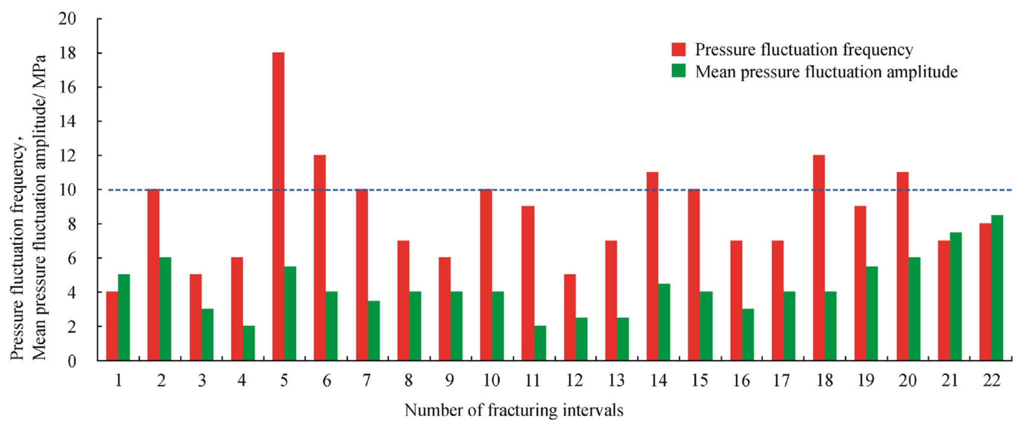

Fig. 5. Statistics of pressure fluctuation frequency and amplitude for 22 intervals in Well P.

By taking four types of pressure curves as an example, Intervals 2, 5, 8 and 18 were selected for collecting the pressure fluctuation frequency and pressure amplitude. The results are shown in Table 3. Fig. 5 shows the statistic results of pressure amplitude fluctuation frequency and pressure amplitude of Interval 22. In summary, far-well fractures are efficiently and widely developed in Intervals 5, 6, 18 and 20, and they are liable to creating complex fractures after fracturing.

3.3. Comprehensive diagnosis of fracture morphology

Combined with shale brittleness and plasticity, typical shale fracturing experiments, and analysis of pressure curve morphology, comprehensive diagnosis of fracture morphology was performed in Well P (Table 4), where the proportion of single fractures reaches 50%. Overall, Types 1 and 2 show good and wide development of fractures, which are liable to form complex fractures, namely, natural bedding seams intersected with hydraulic fractures. Type 3 represents strong plasticity and non-existence of natural fractures, which are likely to form single fractures. Type 4 indicates overall pressure fluctuation inferior to that of Types 1 and 2, showing the possibility of complex fracture formation.

Table 4
Diagnosis result of fracture morphology in Well P.

Fracture morphology	Single fracture	Complex fracture	Fracture network
Fracturing intervals	7–11, 13–16, 21, 22	1, 3, 4, 12, 17–20	2, 5, 6
Proportion	50.0%	36.4%	13.6%

4. Optimization of techniques for improving fracture complexity

The post-fracturing gas production of shale gas well depends on two factors [13–15]: (1) whether the cluster of fracturing interval is located in the high-quality sweet spot; and (2) whether complex fractures are formed after fracturing. Considering the strong heterogeneity and low proportion of complex fractures formed in shale formations, the following techniques should be further applied to improve development performance in the block.

(1) To make fine subsection. First to preliminarily determine the formation brittleness along the wellbore according to the gamma logging data of new wells, then to further optimize the brittle formation with high content of gas and well-developed fractures to be geological sweet spots, and finally make targeted interval and cluster distribution.
(2) To increase the proportion of complex fractures. To properly increase the displacement and viscosity of slickwater, and to take such measures as in sand concentration, timing and slug volume of sand adding, and

alternative injection of fracturing fluid, so as to increase the net pressure in fracturing process.

(3) To learn from the turnaround fracturing technology in the United States. To use this technology to perform temporary plugging in internal fractures and the opening of fractures so as to increase the simulated volume in shale reservoirs.

5. Conclusions

(1) In view of the strong heterogeneity in shale reservoirs, the fracturing curve was employed to identify formation brittleness and plasticity, and then the correlation between natural gamma values and brittleness and plasticity of shale was preliminarily established. The formation with a natural gamma value more than 260 API shows relatively poor brittleness.

(2) Based on the results of large physical simulation experiments, and the statistics of pressure fluctuation frequency and pressure drop of bottomhole pressure curve in the fracturing process, as well as the analytical results of formation brittleness and plasticity, the morphology of fractures was comprehensively diagnosed. In Well P, single fractures, complex fractures, and fracture network account for 50.0%, 36.4% and 13.6%, respectively.

(3) In view of the penetrating trace of horizontal intervals and the situation of fractured wells, some techniques were proposed, including fine subsection of sublayers and improvement of the proportion of complex fractures, so as to increase the effective simulated volume and enhance the development results.

References

[1] Tang Ying, Zhang Jinchuan, Zhang Qin, Long Pengyu. An analysis of hydraulic fracturing technology in shale gas wells and its application. Nat Gas Ind 2010;30(10):33−8.

[2] Chen Shangbin, Zhu Yanming, Wang Hongyan, Liu Honglin, Wei Wei, Luo Yue, et al. Research status and trends of shale gas in China. Acta Pet Sin 2010;31(4):689−94.

[3] Liu Yuzhang, Xiu Nailing, Ding Yunhong, Wang Xin, Lu Yongjun, Dou Jingjing, et al. Multi-factor coupling of hydraulic fracture network in a shale gas reservoir. Nat Gas Ind 2015;35(1):61−6.

[4] Gulen G, Ikonnikova S, Browning J, Tinker S. Fayetteville shale-production outlook. SPE Econ Manag 2014;7(2):47−59.

[5] Guo Xiaozhe, Zhou Changsha. Diffusion seepage model for fractured horizontal well in shale gas reservoir. J Southwest Pet Univ Sci Technol Ed 2015;37(3):38−44.

[6] Ye Dengsheng, Li Jianzhong, Zhu Juhui, Yin Congbin, Xiao Xia, Zhang Juncheng. Practice and prospect of horizontal well fracturing technology in Sichuan shale gas reservoir. Drill Prod Technol 2014;37(3):42−4.

[7] Qian Bin, Zhang Juncheng, Zhu Juhui, Fang Zeben, Kou Shuangfeng, Chen Rui. Application of zipper fracturing of horizontal cluster wells in the Changning shale gas pilot zone, Sichuan Basin. Nat Gas Ind 2015;35(1):81−4.

[8] Soliman MY, East LE, Augustine JR. Fracturing design aimed at enhancing fracture complexity//SPE EUROPEC/EAGE Annual Conference and Exhibition, 14−17 June 2010, Barcelona, Spain. http://dx.doi.org/10.2118/130043-MS.

[9] Wu Qi, Xu Yun, Wang Tengfei, Wang Xiaoquan. The revolution of reservoir stimulation: an introduction of volume fracturing. Nat Gas Ind 2011;31(4):7−12.

[10] Gao Shikui, Zhu Wenli, Yin Cheng. An economic analysis of shale gas resources: a case study of the Marcellus Shale Play. Nat Gas Ind 2014;34(6):141−8.

[11] Jiang Tingxue, Bian Xiaobing, Su Yuan, Liu Shuanglian, Wei Ran. A new method for evaluating shale fractability index and its application. Pet Drill Tech 2014;42(5):16−20.

[12] Jiang Tingxue. A method to calculate bottom hole pressure during fracturing and its application. Nat Gas Ind 1997;17(5):82−4.

[13] Hou Lei, Elsworth D, Sun Baojiang, Wang Jintang. Experimental study on permeability evolution in propped shale fracture. J Southwest Pet Univ Sci Technol Ed 2015;37(3):31−7.

[14] Kennedy RL, Gupta R, Kotov SV, Burton WA, Knecht WN, Ahmed U. Optimized shale resource development: proper placement of wells and hydraulic fracture stages//Abu Dhabi International Petroleum Conference and Exhibition, 11−14 November 2012, Abu Dhabi, UAE. http://dx.doi.org/10.2118/162534-MS.

[15] Willian J, Clarkson CR. Stochastic modeling of two-phase flowback of multi-fractured horizontal wells to estimate hydraulic fracture properties and forecast production//SPE Unconventional Resources Conference, 10−12 April 2013, The Woodlands, Texas, USA. http://dx.doi.org/10.2118/164550-MS.